1

Introduction

1.1 General Introduction

Electrochromism is the phenomenon that describes the optical (absorbance/transmittance/reflectance) change in material via a redox process induced by an external voltage or current [1]. Usually the electrochromic (EC) materials exhibit color change between a colored state and colorless state or between two colors, even multicolor. In nature, its origin is from the change of occupation number of material's internal electronic states. As the core of EC technology, the EC materials have built up many categories during decades of development, for example, according to the coloration type, it could be classified as anodically coloring materials (coloration upon oxidation) or cathodically coloring materials (coloration upon reduction) [2]. Based on the light absorption region in the solar radiation, which consists of these three parts: ultraviolet (UV), visible (Vis), and near-infrared radiation (NIR) lights (Figure 1.1), it could be divided into visible EC materials (wavelength: 380–780 nm), which can be seen by the human eye and therefore are suitable for smart window and indicator applications, and NIR EC materials (wavelength: 780–2500 nm), which have great potential for thermal regulation technologies and even in national defense-related applications [3]. And on the basis of materials species, there are mainly inorganic, organic, and hybrid EC materials [4, 5] (https://commons.wikimedia.org/wiki/File:Solar_spectrum_en.svg). Inorganic EC materials are transition metal oxides (TMOs) (WO_3, NiO, TiO_2, and Prussian Blue [PB]), organic EC materials including small molecules (e.g. viologen), conjugated polymers (e.g. poly(pyrrole), poly(thiophene), and poly(carbazole)) and aromatic polymers (e.g. polyimides [PIs] and polyamides [PAs]), organic–inorganic hybrid materials referring to metallo-supermolecular polymers, and metal–organic framework (MOF). Among them, inorganic materials exhibit excellent long-term stability compared with organic ones; however, considering the structure variety, flexibility, and low-cost solution processability, organic EC materials are superior to inorganic materials. The organic–inorganic hybrid materials are designed to combine advantages of both organic and inorganic materials.

EC materials exhibit color changes during the redox process; therefore the electrochromic devices (ECDs) generally consist of three elements: electrodes, EC materials, and electrolyte solution. The electrodes offer a constant supply of electric

Organic Electronics for Electrochromic Materials and Devices, First Edition. Hong Meng.

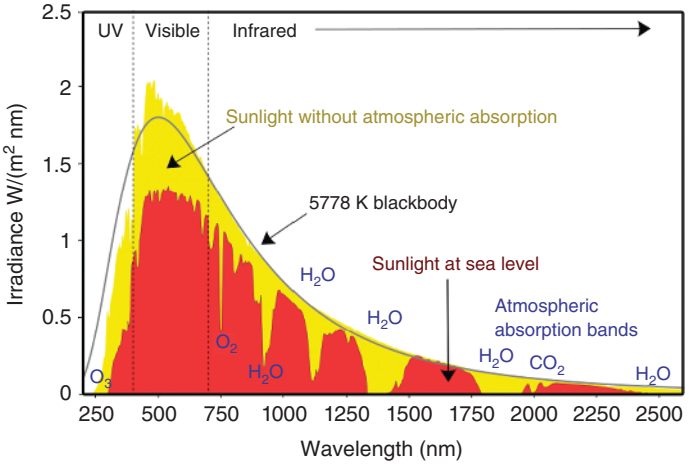

Figure 1.1 Solar irradiance spectrum above atmosphere and at the surface of the Earth. Source: Nick84: https://commons.wikimedia.org/wiki/File:Solar_spectrum_en.svg, Licensed under CC BY-SA 3.0.

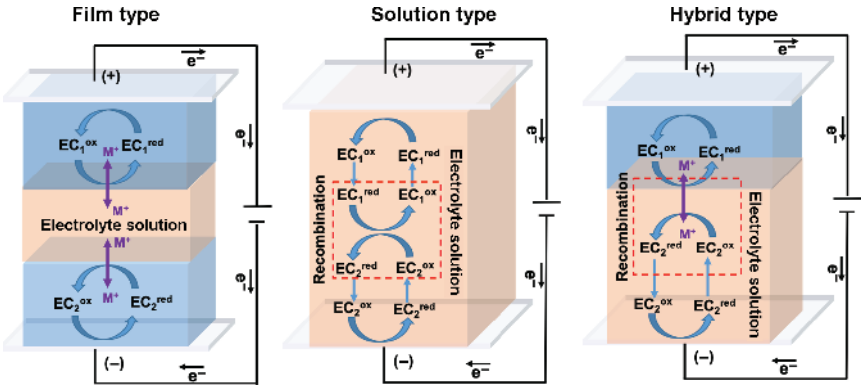

Figure 1.2 The scheme of three types of electrochromic devices.

current, and ions are conducted by the electrolyte solution. Then the EC materials undergo electrochemical oxidation and/or reduction, which results in changes in the optical bandgap and colors. As shown in Figure 1.2, a typical ECD has five layers: two transparent conducting oxide (TCO) layers, EC layer, ion-conducting layer (electrolyte solution), ion storage layer. Particularly, the ion storage layer acts as the "counter electrode" to store ions and keep electric charge balance. And according to the exact state of EC materials, there are three types of ECD: film type (I), solution type (II), and hybrid type (III). The Type I ECD is the most common; many kinds of EC materials are suitable for this type including TMOs, conjugated/non-conjugated polymers, metallo-supermolecular polymers, and MOF/covalent organic framework (COF) materials, which using spin-coating, spray-coating, and dip-coating processes to form uniform films; these films won't dissolute in electrolyte solutions. Type II ECD requires that the EC materials have good solubility in electrolyte

solutions. Therefore many organic small molecules such as viologen, terephthalate derivatives, and isophthalate derivatives are appropriate for this type of device. Meanwhile the fabrication method for this type of device is the most simple one. It just needs to dissolve the electrolyte and EC material in a specific solvent and inject into the prepared conducting cell. Type III ECD uses film-type EC materials as working electrode and solution-type EC materials as ion storage layer.

1.2 The History of Electrochromic Materials

The word "electrochromism" was invented by John R. Platt in 1960 [6], in analogy to "thermochromism" and "photochromism." However, the EC phenomenon could be traced to the nineteenth century, as early as 1815. Berzelius observed the color change of pure tungsten trioxide (WO_3) during the reduction when warmed under a flow of dry hydrogen gas. Then from 1913 to 1957, some patents described the earliest form of ECD based on WO_3 [7, 8]. Therefore the origins of electrochromism are the nineteenth and twentieth centuries. After then, electrochromism technology began to undergo rapid development, especially the exploration of many classes of EC materials. As showed in the technology roadmap (Figure 1.3), we summarized several generations of EC materials during long-term development.

The first-generation EC material is TMOs (e.g. WO_3, NiO, and PB). Among them, WO_3 plays an important role in the electrochromism field; as the first founded EC material, it has already realized commercialization in smart windows application. PB was discovered as a dye by Diesbach in 1704, and then the electrochemical behavior and EC performance of PB was firstly reported by Neff at 1978 [9]. Benefitted from the structure stability and reversible redox process of those inorganic TMOs, the electrochromism based on the thin-film TMOs are widely investigated, including

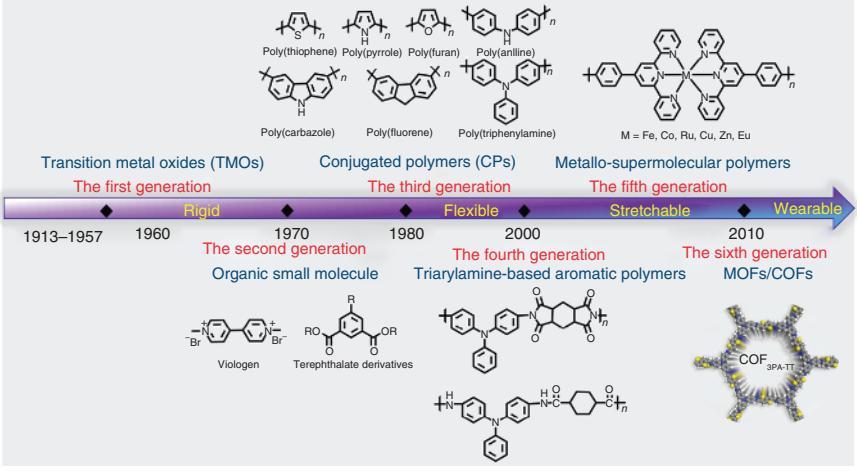

Figure 1.3 The roadmap of EC materials development.

the development of new TMOs materials, introduction of new nanostructures, and different element doping.

Following the first-generation TMO EC materials, organic small molecule EC materials have emerged since 1970. Among them, viologen as the most representative small molecule was first discovered by Michaelis and Hill in 1932 [10], and because of the violet on the reduction, these 1,1′-disubstituted-4,4′-bipyridine compounds were named "viologen." Then in 1973, Shoot made a new flat alphanumeric display using heptyl viologen; this can be regarded as the beginning of the use of viologen for electrochromism [11]. After a century's development, viologen already has been successfully commercialized. Besides the viologen, other small molecules EC materials such as terephthalate derivatives, isophthalate derivatives, methyl ketone derivatives, and some dye molecules have also attracted much attentions from scientists due to their simple structure and low cost.

The third-generation EC materials are conjugated polymers. In 1983, Francis Garnier and coworkers firstly characterized the EC properties of a series of five-membered heterocyclic polymers including poly(pyrrole), poly(thiophene), poly(3-methylthiophene), poly(3,4-dimethylthiophene), and poly(2,2′-dithiophene). Since then, conjugated polymers were given rise to the rapid emerge as a new class of electrochromism [12]. Five years later, Berthold Schreck observed the electrochromism phenomenon of poly(carbazole), which showed a color change from pale yellowish to green together with the conductivity enhancement [13]. To date, the conjugated polymer EC system has been well developed, from better understandings on mechanisms to completed color pallette with soluble or electro-deposited polymers, and even full-color display samples or roll-to-roll fabricated flexible devices.

Later, in early 2000, triarylamine (TA)-based aromatic polymers especially the PIs and PAs have drawn considerable attention from the research community as the fourth-generation EC materials. The correlation between electrochemical properties and chemical structures of different aromatic PIs was firstly described in 1990. Ten years later, Zhiyuan Wang and coworkers [14] reported the first EC behavior of poly(ether naphthalimide)s, which showed stepwise coloration process, from colorless to red and to dark blue corresponding to the neutral, radical anion, and dianion species, respectively. However, due to the high rigidity of the PIs/PAs backbone and strong intermolecular interactions, the poor processability limited the development of PIs or PAs EC materials. Therefore the TA groups were introduced to the PIs/PAs backbone to improve the solubility of aromatic polymers. The first TA-based polyamide PA was synthesized in 1990 [15], and the first aromatic polyimides integrating interesting EC properties containing TA groups were disclosed in 2005 [16]. Since then, Liou, Hsiao and, other groups have developed numerous TA-based EC PIs/PAs. Most of the PIs/PAs were solution processible and thermally stable with excellent adhesion with indium tin oxide-coated glass electrode and had good electrochemical stability. Now the TPA-based PIs/PAs are considered as great anodic EC materials due to proper oxidation potentials, electrochemical stability, and thin-film formability.

Benefiting from the bloom and revolution of organic polymers, metallo-supermolecular polymers were developed by incorporating metal centers into synthetic polymer chains, as the fifth-generation EC materials. The first metal-containing polymer, poly(vinyl-ferrocene), was reported in as early as 1955 [17]. However, due to the insolubility of those macromolecules and the limitation of characteristic technologies in the early years, the metallo-supermolecular polymers haven't been rapidly developed until the mid-1990s [18]. Since then, metallo-supermolecular polymers began to be widely explored in EC field with the advantages of beneficial properties of both organic and inorganic materials. Especially, because the transition metal complexes often exhibit well-defined redox events and intense charge transfer transitions in the NIR region, metallo-supermolecular polymers often show potentials in NIR EC application.

More recently, with the active researches on the crystalline and porous MOFs and COFs, the sixth-generation MOFs/COFs EC materials have emerged. In 2013, the first EC properties of MOFs using naphthalene diimide (NDI) as organic linker were reported by Professor M. Dinca's group [19]. And the first COFs EC material using the TPA as building block was revealed by Yuwu Zhong and Dong Wang and coworkers in 2019 [20]. All in all, some essential features of MOFs/COFs give them advantages in EC, including designable and precise molecular structure, simple self-assembly synthesis, and porous structure that facilitate the electrolyte ions transport. However, these new EC materials haven't been fully revealed; many efforts should be taken to improve the device performance of MOFs/COFs-based electrochromism.

1.3 The Key Parameters of Electrochromism

In order to elucidate the EC properties of EC materials, in situ UV–Vis–NIR spectroelectrochemistry (SEC) measurements were performed on a spectrophotometer, combining with an electrochemical workstation to apply and control the potential in the SEC cell. This SEC spectrum dynamically records the absorption change of EC materials during different applied voltage, which reflects the color change during the whole redox process. As an example, the SEC of a black-to-transmissive EC material is shown in Figure 1.4. Both absorbance model and transmittance model could be used to carry out the SEC measurement.

1.3.1 Electrochromic Contrast

EC contrast ($\Delta\%T$) is measured as the percent transmittance change of the EC material at a specific wavelength [22] it is a primary parameter for characterizing the EC materials. It is calculated from the difference of light transmission (TM) in the bleached and colored state TM_b and TM_c at the specified wavelength. And the transmittance values are generally recorded upon the application of square-wave potential steps to the electroactive film placed in the beam of a spectrophotometer. Each color has a characteristic wavelength as shown in Figure 1.5b, such as the

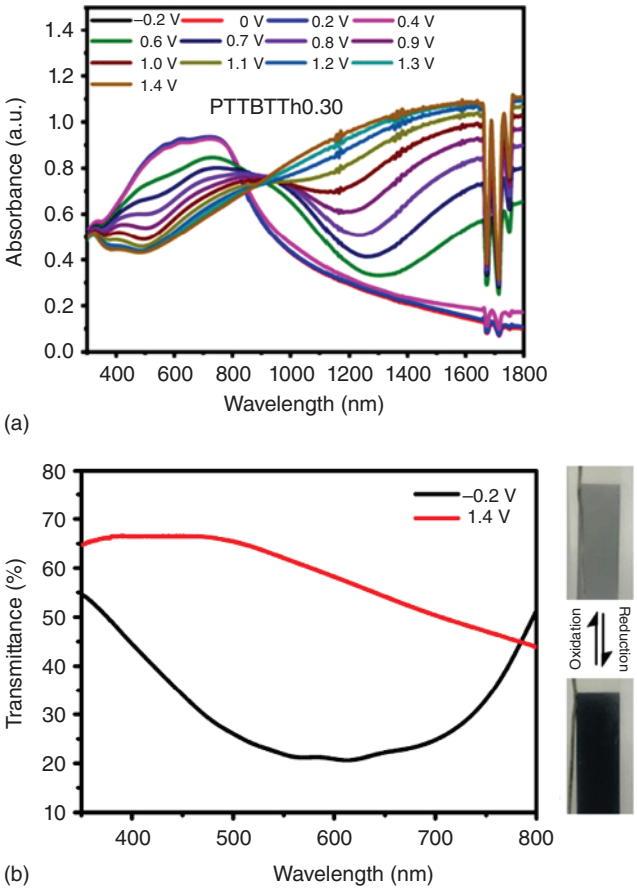

Figure 1.4 The spectroelectrochemistry (SEC) of a black-to-transmissive EC material. (a) Absorbance model and (b) transmittance model. Source: Reproduced by permission Li et al. [21]. © 2018, Royal Society of Chemistry.

wavelength of blue color is ranging from 455 to 490 nm. Therefore, in most cases, the contrast in the characteristic wavelength is chosen to evaluate the degrees of color change. Usually the absorption of this characteristic wavelength also reaches its maximum value (λ_{max}). Moreover, there is evidence that human eyes are most sensitive to green light with a wavelength of 555 nm [25]. It's also recommended to calculate the contrast in 555 nm for comparison in different publications. Specifically, a contrast test example is shown in Figure 1.5a, the TM_b and TM_c of λ_{max} 425 nm are 1% and 99%, respectively; therefore the $\Delta\%T$ is calculated as 98%. For applications such as smart windows, in which the difference between the bleached and colored states is expected to be the highest, the $\Delta\%T$ should be higher than 80%. Many inorganic EC materials, organic small molecules, and PEDOT series polymers, which have a high transmittance in the bleached state, can achieve this index. Especially, some reported small molecule EC materials even show $\Delta\%T$ exceed 95% [23].

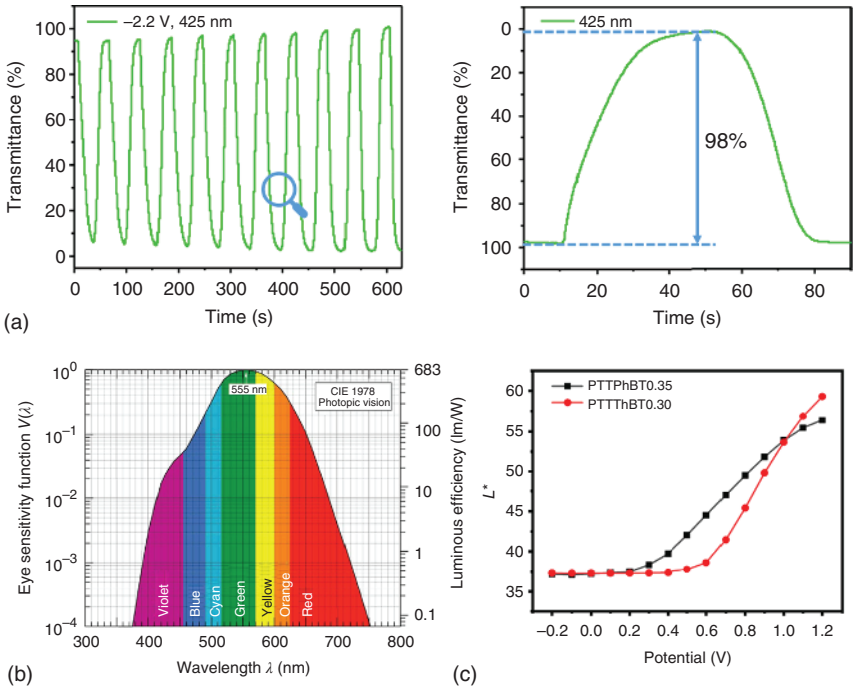

Figure 1.5 (a) The electrochromic contrast of a small molecule EC material. Source: Jiang et al. [23], (b) sensitivity function of the human eye $V(\lambda)$ and luminous efficacy vs wavelength. Source: Fred Schubert [24]. © 2006, Cambridge University Press. (c) The change of the lightness values from the neutral to the oxidized states. Source: Li et al. [21]. © 2018, Royal Society of Chemistry.

Meanwhile, for some broad absorption or color-to-colorless EC materials, measurements on the relative luminance change ($\Delta\%Y$) during an EC switch are more realistic for exhibiting the overall EC contrast, which conveys more information on the perception of transmittance to the human eye. As an example, a luminance change curve during the redox process of black-to-transmissive EC materials is shown in Figure 1.5c. The lightness L^* value (from 0 (black) to 100 (white)) of 37.5 (black state) increases to 60 (bleach state); therefore the $\Delta\%Y$ is calculated as 22.5%.

Except for the aforementioned method for electrochemical contrast measurements, a photopically weighted value called photopic contrast was proposed by Javier Padilla et al. [26]. The photopic contrast also reflects an overall contrast during the whole visible region, which is more consistent with the real application condition. It can be calculated using the following equation:

$$T_{\text{photopic}} = \frac{\int_{\lambda_{\min}}^{\lambda_{\max}} T(\lambda)S(\lambda)P(\lambda)\mathrm{d}\lambda}{\int_{\lambda_{\min}}^{\lambda_{\max}} S(\lambda)P(\lambda)\mathrm{d}\lambda}$$

where T_{photopic} is the photopic transmittance, $T(\lambda)$ is the spectral transmittance of the device, $S(\lambda)$ is the normalized spectral emittance of a 6000 K blackbody, and $P(\lambda)$

is the normalized spectral response of the eye. λ_{min} and λ_{max} define the considered range of wavelengths.

1.3.2 Switching Time

In the context of electrochromism, the switching time (t) can be defined as the time needed for EC materials to switch from one redox state to the other. It is generally followed by a square wave potential step method coupled with optical spectroscopy. Switching time depends on several parameters, such as the ability of the electrolyte to conduct ions as well as the ease of intercalation and deintercalation of ions across the EC active layer, the electrical resistances of electrolytes, and the transparent conducting films. Usually the liquid electrolyte has a lower resistance than the solid electrolyte; therefore the half device and the liquid electrolyte ECD will exhibit a rapid switching than solid ECD. Meanwhile, the large area ECD such as the large smart windows will show a lower switching compared with the small laboratory samples due to the larger electrical resistances of transparent conducting films. However, fast switching is not required in all applications, such as the switchable window technologies; the obvious color change process will increase the fun of user experience. Conversely, the sub-second magnitude rapid switching is particularly desired for display applications.

Usually the switching times are evaluated at the λ_{max} or 555 nm together with the EC contrast. Therefore there are two kinds of switching time. One is electrochemical switching time, as shown in Figure 1.6a, which is the time required for the current density to change by 90% or 95% between two constant voltages. Meanwhile the switching time of oxidization ($t_{oxidization}$) and reduction ($t_{reduction}$) process can be estimated from this curve. The other is optical switching time (Figure 1.6b), which defines the time needed for the transmittance to change by 90% or 95%. Correspondingly, the coloration switching time ($t_{coloration}$) and bleaching switching time ($t_{bleaching}$) are recorded in this measurement. It is worth noting that the pulse length of potential step has influence in transmittance. A shorter potential step will achieve a smaller contrast, and longer potential will allow EC materials to reach stationary transmittance value in both coloration and bleaching state. But after a certain length, continuing increase the pulse length won't boost the contrast. Therefore the pulse length that just reached the highest contrast are applied to switching time as well as contrast tests.

However, the aforementioned method of switching time is an experiential measurement, which has a difference in varied research groups, such as the different percentage of transmittance change (90% or 95%). Therefore, it is difficult to compare switching time data between different research groups. In recent years, Javier Padilla and coworkers proposed a standard method for calculating EC switching times. They fitted the contrast values as a function of pulse length to the following exponential increase function:

$$\Delta TM(t) = \Delta T\mathrm{M}_{max}(1 - \mathrm{e}^{-t/\tau})$$

where ΔT_{max} represents the full-switch contrast obtained for long pulse lengths and τ is the time constant. If switching time t is equal to τ, 63.2% of the maximum

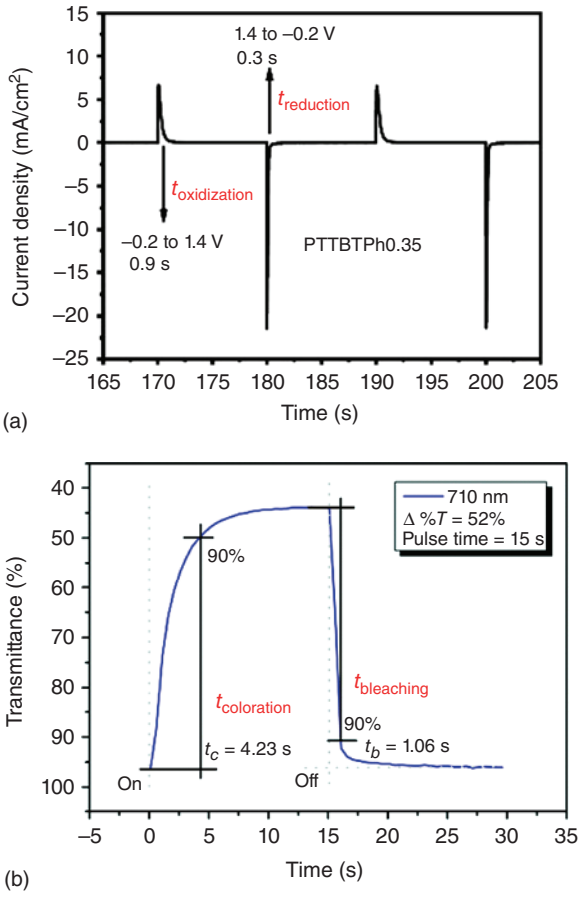

Figure 1.6 The switching time of EC materials. (a) Electrochemical switching time. Source: Li et al. [21]. © 2018, Royal Society of Chemistry (b) Optical switching time. Source: Hsiao et al. [27].

transmittance change is reached. At a time of 2.3τ, 90% ΔTM_{max} is switched, identically 95% and 99% of ΔTM_{max} corresponding to 3τ and 4.6τ.

Therefore, for new EC materials, the same chronoabsorptometric responses [28] should be measured and fitted to the aforementioned function. From the fittings, the max values of ΔTM_{max} (the contrast corresponding to a full switch), the time constant τ, and the corresponding regression coefficient r^2 will be obtained. Afterwards the switching time $t_{90\%}$ or $t_{95\%}$ will be easily calculated. This method allows an easy direct comparison between different reported values.

1.3.3 Coloration Efficiency

Coloration efficiency (CE) plays a fundamental role in the evaluation of the efficiency of charge utilization during the EC processes. It relates the optical absorbance change of an EC material at a given wavelength (ΔA) to the density of injected/ejected electrochemical charge necessary to induce a full switch (Q_d). The higher CE value indicates a large transmittance change with a small amount of charge, which makes more effective use of the injected charge. CE value can be

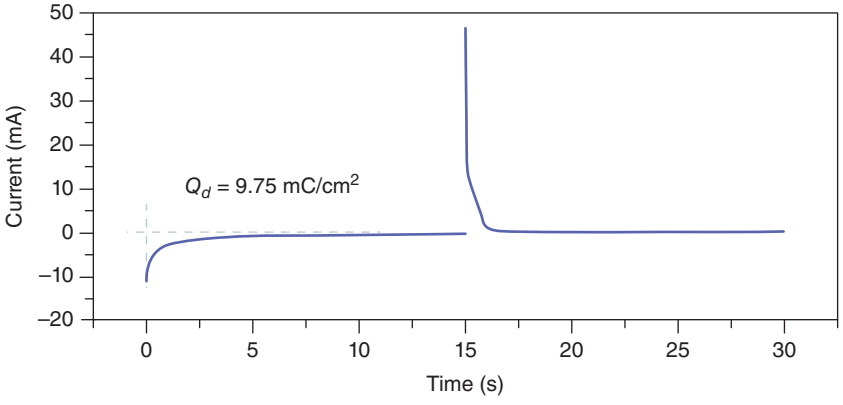

Figure 1.7 The calculation of Q_d. Source: Hsiao et al. [27].

calculated using the following equation:

$$\mathrm{CE} = \frac{\Delta A}{Q_d} = \frac{\log\left(\frac{T_{ox}}{T_{neut}}\right)}{Q_d}$$

where T_{ox} and T_{neut} are the transmittances in the oxidized and neutral states, respectively, and Q_d represents the injected/ejected charge per unit area, which could be obtained from the integral area of the current density curve during voltage switching (Figure 1.7).

Very similar to the previous parameters contrast and switching time, the CE values are also different depending on the selective wavelength, as shown in Figure 1.8. Several kinds of CE value of the same EC materials are exhibited: in most reported literature, the CE of characteristic wavelength reaching the maximum contrast (λ_{max}) is calculated, which is the maximum CE value (CE_{max}). Also, the CE value at 555 nm

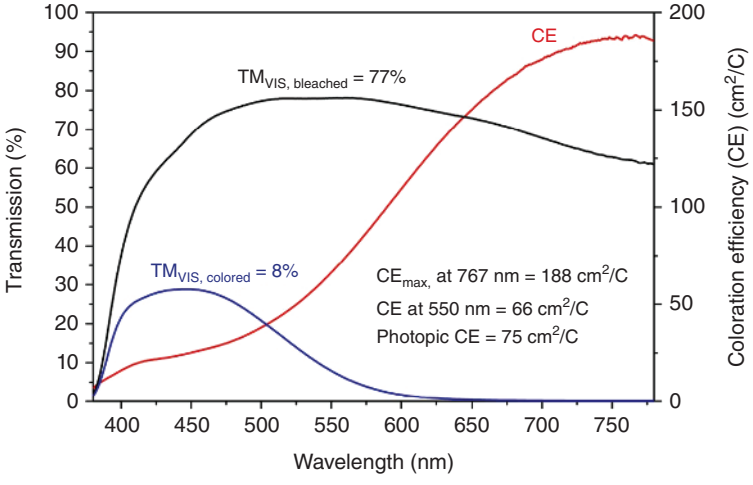

Figure 1.8 Different types of CE value of the same EC materials. Source: Kraft [25].

is calculated for comparison in different publishes because of the highest sensitivity of human eyes at 555 nm as well as the photopic CE based on the photopic transmittance mentioned in the contrast part, which considered the light transmission over the wavelength range between 380 and 780 nm normalized with the spectral sensitivity of the human eye. Therefore, more plot of CE values should be obtained rather than single-valued CE values, to give more information about the performance of EC materials.

In addition, when insightfully considering the injected/ejected charge Q_d, we can find it in fact to consist of three part: faradaic charge Q_F associated with doping/de-doping, capacitive charge Q_C due to the capacitive nature of the ECD, and parasitic charge Q_P associated with electrolyte/impurity reactions. Among them, the faradaic charge is the source of redox activity leading to chromic change actually. Therefore, Fabretto et al. reported a new technique for measuring CE by extracting the faradaic charge from the total charge and calculated the only faradaic charge-based CE value [29]. As we discussed, the total charge flow is simply the addition of the three individual charge flows and is given by

$$Q_d = Q_F + Q_C + Q_P$$

where the parasitic current was a small component (approximately <2%) compared with the other two and therefore can be ignored. Then the time–evolution total current flow can be described as following:

$$I_d(t) = I_F(t) + I_C(t) = \frac{n\mathrm{FAC}_0 D^{1/2}}{\pi} t^{-1/2} + I_0 \mathrm{e}^{-t/\mathrm{RC}} = k\, t^{-1/2} + I_0 \mathrm{e}^{-t/\mathrm{RC}}$$

where n is the number of electrons transferred per molecule, F is the Faraday constant (96 500 C/mol), A is the electrode area (cm^2), C_0 is the concentration of species in the bulk solution (mol/cm^3), D is the apparent diffusion coefficient (cm^2/s), t is time in seconds, I_0 is the maximum current flow at $t = 0$, R is the cell resistance, and C is the double layer capacitance. Then fitting the experimental data to this equation and substituting the constant k, at last, a plot of the time–evolution faradaic current will be obtained, and the corresponding faradic-corrected CEs can be calculated. Usually, the faradic-corrected CEs are larger than the uncorrected results, because the total charge ingress/egress (i.e. Q_d) is larger than the faradic charge (i.e. QF).

1.3.4 Optical Memory

The optical or EC memory (also called open-circuit memory) of an EC material can be defined as the propensity of the material to retain its redox/colored state upon removing the external bias. Usually, the memory effect are often observed in film-state EC materials such as conjugated polymers, which well adhered onto the electrode, and hence restrict the movement of the electrons. In contrast, some solution-based ECDs (e.g. viologens) will exhibit a self-erasing effect, which means the colored state disappeared rapidly in the absence of applied voltage because the electrons diffuse freely in this type of device. The memory effect is useful for the energy-saving devices and also can be applied for data storage. Figure 1.9 shows

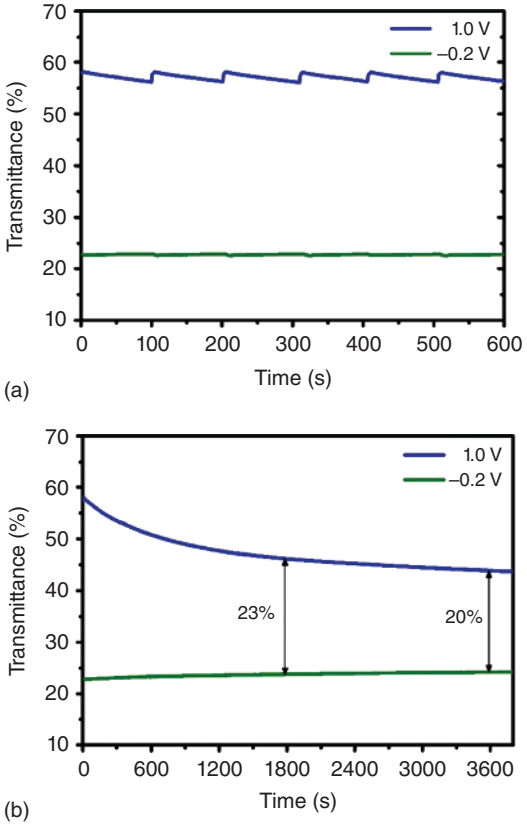

Figure 1.9 Open-circuit memory tests of PBOTT-BTD spray coated on an ITO-coated glass slide in 0.1 M TBAPF6/ACN at 423 nm: (a) short- and (b) long-term performance. Source: Li et al. [21].

an optical memory test. The short-term memory was investigated by applying a potential pulse for 2 seconds prior to forming the open-circuit state for 100 seconds; the transmittance change at 423 nm was monitored simultaneously (Figure 1.9a). Then a long-term memory is also studied by applying a potential for two seconds and removing the bias for one hour (Figure 1.9b). The EC conjugated polymers remain in the initial transmittance contrast well in the absence of an applied voltage, which exhibits a good optical memory.

1.3.5 Stability

In most cases of laboratory study, researchers record the number of redox cycles that an EC material stand without significant loss in the performance as the electrochemical stability, irreversible oxidation or reduction at extreme potentials, side reactions with water or oxygen, and heat release in the system during switches may cause the degradation of electrochemical stability. Usually, the charge density Q_d recorded under electrochemical cycling is up to 10^4–10^6, as shown in Figure 1.10a. The charge density of a Ti-doped V_2O_5 EC film haven't changed through 2×10^6 cycles; meanwhile the transmittance change at a certain wavelength during continuous cycling is also important to describe the stability

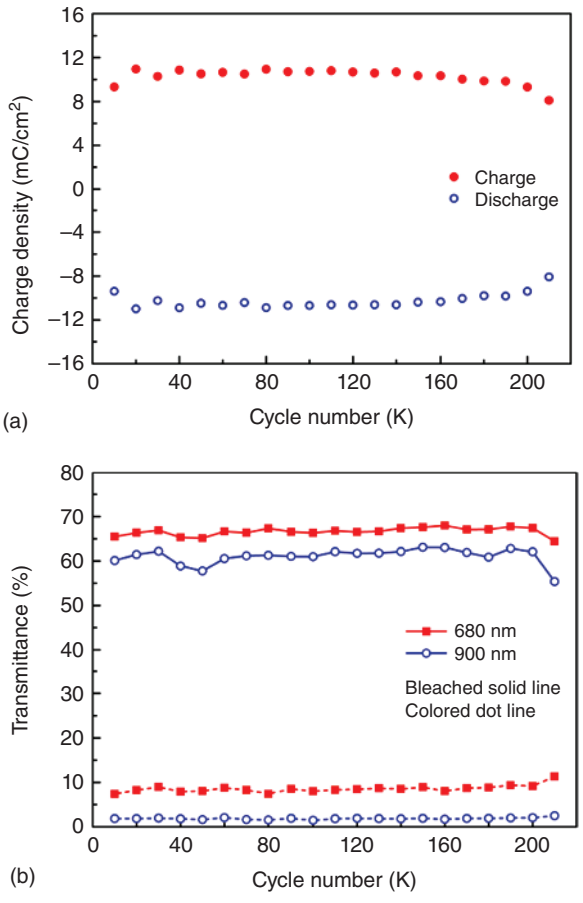

Figure 1.10 Charge density (a) and transmittance (b) variation curves of ECD with the cycle number K :1000. Source: Wei et al. [30].

of an EC material. Such as shown in Figure 1.10b, the transmittance of the ECD remains stable through 200 000 cycles. Actually, the CE change after numerous cycles also can be used to evaluate the long-term stability of EC materials, because it contains information of both transmittance and charge density.

However, if we consider the real application of ECD in building windows, there are more strict conditions for durability and reliability. For instance, a lifetime over 20 years with more than 10^6 switching cycles is necessary. Extreme weather conditions such as temperatures below −20 °C and above +40 °C are huge challenge for both EC materials and electrolytes, as well as other degradation factors such as high solar irradiation levels, fast temperature changes, uneven temperature distribution and additional stresses, rain, humidity, mechanical shock, and drying. Therefore, in 1998, Carl M. Lampert proposed a standard test guideline for industry application of EC [31], as shown in Figure 1.11. Recently, the International Organization for Standardization (ISO) also has launched an international standard: Glass in building – Electrochromic glazings – accelerated aging test and requirements (ISO 18543) for EC use in buildings.

EC color/bleach cycling	1. 25 000 cycles at 25 °C 2. 10 000 cycles at – 20 °C 3. 25 000–100 000[b] cycles with UV[a] at 65 °C
UV[a] stability	Prolonged cycles (12 h colored, 12 h bleach) for a total exposure of 6000 MJ/m^2, UV intensity integrated between 300 and 400 nm
Heat storage	500 h at 90 °C
Low temperature storage	1000 h at 20 °C to – 30 °C
Humidity/temperature storage	1000 h at 70 °C, 90% humidity
Thermal cycling	85 °C for 4 h, followed by – 40° C for 4 h and followed by 37 °C for 16 h at 100% R.H. (4 h of ramp between each condition) (repeat four times)
Thermal shock	One hour colored and one hour bleached. Test in a UV chamber, with UV[a] lamp on during coloration. Spray with 25 °C water in bleached state (24 cycles)

[a]Black panel temperature during the bright periods of 60 °C, and 25 °C in the dark periods.
[b]Asahi has used up to 100 000 cycles.

Figure 1.11 Recommended testing guidelines for EC windows for exterior architectural applications. Source: Lampert et al. [31].

1.4 Conclusion

In this chapter, a broad overview of electrochromism, EC materials, device structure, development history, and key parameters of electrochromism have been introduced briefly. More detailed descriptions of each area will be discussed in Chapters 2–15. In summary, research in EC technologies has achieved significant breakthroughs over the decades. Many generations of EC materials have been developed, ranging from traditional metal oxides to more recent organic polymers, small molecules, and hybrid materials. Moreover, benefit from the ECD design and structural optimization, flexible substrate-based devices were fabricated with the low-price roll-to-roll process, which makes the EC technology have large scope applications, such as smart windows for reducing building energy consumption, self-powered EC window using organic photovoltaic cells as power supplement, car rear-view mirrors for greater safety, and smart sunglasses for better UV-radiation protection. Many of these technologies and applications have been commercialized and are available on the market. With the concerted efforts of researchers and engineers, we believe that the new EC materials and advanced technologies will constantly develop and more advanced ECD with low manufacturing cost will be exploited to realize practical applications.

References

1 Fletcher, S. (2015). The definition of electrochromism. *Journal of Solid State Electrochemistry* 19 (11): 3305–3308.
2 Camurlu, P. (2014). Polypyrrole derivatives for electrochromic applications. *RSC Advances* 4 (99): 55832–55845.
3 Wang, Z., Wang, X., Cong, S. et al. (2020). Fusing electrochromic technology with other advanced technologies: a new roadmap for future development. *Materials Science & Engineering R: Reports* 140.

4 Wu, W., Wang, M., Ma, J. et al. (2018). Electrochromic metal oxides: recent progress and prospect. *Advanced Electronic Materials* 4 (8).

5 Mortimer, R.J. (2011). Electrochromic materials. *Annual Review of Materials Research* 41 (1): 241–268.

6 Platt, J.R. (1961). Electrochromism, a possible change of color producible in dyes by an electric field. *The Journal of Chemical Physics* 34 (3): 862–863.

7 Hutchison, M.R. (1913). Electrographic display apparatus and method. US Patent 1,068,774, filed 29 July 1913.

8 Lehovec K. (1957). Photon modulation in semiconductors. US Patent 2,776,367, filed 1 January 1957.

9 Neff, V.D. (1978). Electrochemical oxidation and reduction of thin-films of prussian blue. *Journal of the Electrochemical Society* 125 (6): 886–887.

10 Michaelis, L. and Hill, E.S. (1933). The viologen indicators. *The Journal of General Physiology* 16 (6): 859–873.

11 Schoot, C.J., Ponjee, J.J., van Dam, H.T. et al. (1973). New electrochromic memory display. *Applied Physics Letters* 23 (2): 64–65.

12 Garnier, F., Tourillon, G., Garzard, M., and Dubois, J.C. (1983). Organic conducting polymers derived from substituted thiophenes as electrochromic material. *Journal of Electroanalytical Chemistry* 148: 299–303.

13 Mengoli, G., Musiani, M.M., Schreck, B., and Zecchin, S. (1988). Electrochemical synthesis and properties of polycarbazole films in protic acid media. *Journal of Electroanalytical Chemistry and Interfacial Electrochemistry* 246 (1): 73–86.

14 Zheng, H.B., Lu, W., and Wang, Z.Y. (2001). Electrochemical and electrochromic properties of poly(ether naphthalimide)s and related model compounds. *Polymer* 42 (8): 3745–3750.

15 Oishi, Y., Takado, H., Yoneyama, M. et al. (1990). Preparation and properties of new aromatic polyamides from 4,4′-diaminotriphenylamine and aromatic dicarboxylic acids. *Journal of Polymer Science Part A: Polymer Chemistry* 28 (7): 1763–1769.

16 Cheng, S.-H., Hsiao, S.-H., Su, T.-H., and Liou, G.-S. (2005). Novel aromatic poly(amine-imide)s bearing a pendent triphenylamine group: synthesis, thermal, photophysical, electrochemical, and electrochromic characteristics. *Macromolecules* 38 (2): 307–316.

17 Arimoto, F.S. and Haven, A.C. (1955). Derivatives of dicyclopentadienyliron. *Journal of the American Chemical Society* 77 (23): 6295–6297.

18 Whittell, G.R. and Manners, I. (2007). Metallopolymers: new multifunctional materials. *Advanced Materials* 19 (21): 3439–3468.

19 Wade, C.R., Li, M., and Dincă, M. (2013). Facile deposition of multicolored electrochromic metal–organic framework thin films. *Angewandte Chemie International Edition* 52 (50): 13377–13381.

20 Hao, Q., Li, Z.-J., Lu, C. et al. (2019). Oriented two-dimensional covalent organic framework films for near-infrared electrochromic application. *Journal of the American Chemical Society* 141 (50): 19831–19838.

21 Li, W., Ning, J., Yin, Y. et al. (2018). Thieno[3,2-*b*]thiophene-based conjugated copolymers for solution-processable neutral black electrochromism. *Polymer Chemistry* 9 (47): 5608–5616.

22 Beaujuge, P.M. and Reynolds, J.R. (2010). Color control in π-conjugated organic polymers for use in electrochromic devices. *Chemical Reviews* 110 (1): 268–320.

23 Jiang, M., Sun, Y., Ning, J. et al. (2020). Diphenyl sulfone based multicolored cathodically coloring electrochromic materials with high contrast. *Organic Electronics* 83: 105741.

24 Fred Schubert, E., Chapter 16. *Human Eye Sensitivity and Photometric Quantities in Light-Emitting Diodes*, 2e. Cambridge University Press.

25 Kraft, A. (2018). Electrochromism: a fascinating branch of electrochemistry. *ChemTexts* 5 (1): 1–18.

26 Padilla, J., Seshadri, V., Filloramo, J. et al. (2007). High contrast solid-state electrochromic devices from substituted 3,4-propylenedioxythiophenes using the dual conjugated polymer approach. *Synthetic Metals* 157 (6–7): 261–268.

27 Hsiao, S.-H. and Lin, S.-W. (2016). Electrochemical synthesis of electrochromic polycarbazole films from *N*-phenyl-3,6-bis(*N*-carbazolyl)carbazoles. *Polymer Chemistry* 7 (1): 198–211.

28 Hassab, S., Shen, D.E., Österholm, A.M. et al. (2018). A new standard method to calculate electrochromic switching time. *Solar Energy Materials and Solar Cells* 185: 54–60. https://doi.org/10.1016/j.solmat.2018.04.031.

29 Fabretto, M., Vaithianathan, T., Hall, C. et al. (2008). Faradaic charge corrected colouration efficiency measurements for electrochromic devices. *Electrochimica Acta* 53 (5): 2250–2257.

30 Wei, Y., Zhou, J., Zheng, J., and Xu, C. (2015). Improved stability of electrochromic devices using Ti-doped V_2O_5 film. *Electrochimica Acta* 166: 277–284.

31 Lampert, C.M., Agrawal, A., Baertlien, C., and Nagai, J. (1999). Durability evaluation of electrochromic devices – an industry perspective. *Solar Energy Materials and Solar Cells* 56 (3): 449–463.